

# Use of binding energy in comparative molecular field analysis of isoform selective estrogen receptor ligands

Peter Wolohan, David E. Reichert\*

*Mallinckrodt Institute of Radiology, Washington University School of Medicine, 510 S. Kingshighway Blvd., Campus Box 8225, St. Louis, MO 63110, USA*

Received 18 July 2003; received in revised form 29 December 2003; accepted 3 March 2004

Available online 27 April 2004

## Abstract

A diverse set of 30 estrogen receptor ligands whose relative binding affinities (RBA) with respect to 17 $\beta$ -estradiol were available in both isoforms of the nuclear estrogen receptor (ER $\alpha$ , ER $\beta$ ) were studied with a combination of comparative molecular field analysis (CoMFA) and binding energy calculations. The ligands were docked inside the ligand-binding domain (LBD) of both ER $\alpha$  and ER $\beta$  utilizing the docking program Gold. The binding energy ( $\Delta E$ ) and corresponding non-bonded interactions (NB) of the subsequent protein–ligand complexes were calculated in both the gas-phase and implicit aqueous solution using the generalized born surface area (GB/SA) model. A partial least-squares analysis of the calculated energies indicated that the NB<sub>(g)</sub> were sufficiently predictive in ER $\alpha$ , but performed poorly in ER $\beta$ . Further analysis of the calculated energies by dissecting the ligands into two distinct classes, estrogen-like and heterocyclic, yielded more predictive models. In particular the  $\Delta E$  calculated in solution proved particularly predictive for the estrogen-like ligands in ER $\beta$ . Finally the estrogen subtype selective nature RBA (ER $\alpha$ /ER $\beta$ ) of a test-set consisting of six of the original ligands was predicted. The combined CoMFA and non-bonded interaction energy model ranked correctly the ligands in order of increasing RBA (ER $\alpha$ /ER $\beta$ ), illustrating the utility of this method as a prescreening tool in the development of novel estrogen receptor subtype selective ligands.

© 2004 Elsevier Inc. All rights reserved.

**Keywords:** Estrogen; Subtype selective; CoMFA; Binding energy

## 1. Introduction

Estrogens play a critical role in the growth, development and sustenance of a wide range of tissues. Predominantly formed in the reproductive organs of the human body, specifically the ovaries and testis, estrogens infiltrate many cells in the body. They play a critical role in the physiology of the female reproductive system, the maintenance of bone density and cardiovascular health.

In addition to the endogenous estrogens many synthetic chemicals used in industry and agriculture, such as polychlorinated hydroxybiphenyls (PCBs), insecticides and herbicides, have been reported as exhibiting estrogenic responses in various species [1,2]. Furthermore a diverse group of natural compounds, the phyto-estrogens, are produced by plants as bactericidal and fungicidal agents.

These phyto-estrogens represent a natural reservoir of estrogenic compounds that may affect both human and animal species. Their presence in the food chain may be a beneficial source of estrogens which counter the threat of the development of reproductive cancers such as breast and prostate cancer [3].

The estrogen receptor (ER) is the natural target of these ligands. This is a member of the nuclear hormone receptor gene superfamily and functions as a ligand activated transcription factor. The receptor possesses two conserved domains, the DNA binding domain, and the ligand binding domain which also controls the transcription functions. As a result of the far reaching role of estrogens in the physiology of both humans and animal species the estrogen receptor represents a viable and important pharmaceutical target. In particular it is a target for pharmaceutical agents for hormone replacement in menopausal women, reproductive cancers such as breast cancer, uterine cancer and prostate cancer.

\* Corresponding author. Tel.: +1-314-362-8461; fax: +1-314-362-9940.  
E-mail address: [reichertd@wustl.edu](mailto:reichertd@wustl.edu) (D.E. Reichert).

Pharmaceuticals developed to date can be divided into three distinct categories. The first category acts solely as receptor agonists such as the estrogen receptors natural ligand 17 $\beta$ -estradiol. The second category includes antiestrogens such as the compound ICI 164,384 and act as pure antagonists. The third category includes antiestrogens which have the ability to act as both agonists or antagonists, this includes such compounds as tamoxifen and LY117018 [4].

In 1996 a new isoform of the estrogen receptor (ER $\beta$ ) was discovered [5,6]. The possibility that the tissue selectivity and function of certain estrogens and antiestrogens was due to their specificity for either the classical ER $\alpha$  or the newly discovered isoform has been validated by recent studies concerning the difference in tissue distribution between the two estrogen receptor isoforms [5,7,8]. In addition it has been reported that the pharmacology of several classical estrogen receptor agonists and antagonists is reversed for ER $\beta$  [9,10].

In the most part the subtype-selectivity of the classical estrogens and antiestrogens developed to date has been modest [7]. As a result there exists the opportunity to develop novel subtype-selective ligands which would target the physiological role of either the ER $\alpha$  or ER $\beta$  receptor with greater specificity. Recent reports in the literature have focused on a series of nonsteroidal compounds based on substituted furans and pyrazoles [11–13]. These compounds have been shown to exhibit unprecedented estrogen subtype selectivity compared to the classical steroidal compounds. In particular the compound 4-propyl-1,3,5-triphenolpyrazole (PPT) has been reported to have 400-fold affinity for the ER $\alpha$  isoform of the estrogen receptor. It is this new class of compounds that is the subject of this study; if we can understand from a fundamental basis the nature of their increased subtype selectivity it may be possible to develop more potent and selective compounds for these important pharmaceutical targets. In this effort we report a study combining ligand receptor docking, molecular mechanics evaluation of the intermolecular interaction energies, and CoMFA for both ER $\alpha$  and ER $\beta$ .

Comparative molecular field analysis (CoMFA) is a computational technique which has been utilized extensively to study the relationship between three-dimensional molecular information such as steric and electrostatic fields and biological activity [14–17]. CoMFA is based on the premise that the pharmacophoric elements which are responsible for the biological activity of a compound, be it favorable or unfavorable, will be represented in the calculated steric and electrostatic field of the compound. By studying a series of compounds, called the training set, consisting of compounds with good, medium and poor bioactivity for a specific protein target it is possible to extrapolate a three-dimensional pharmacophoric model that explains the observed bioactivity. Indeed this model suggests how the steric and electrostatic fields might be manipulated to produce a novel compound with enhanced bioactivity. One requirement of CoMFA is that the

compounds in the training set be aligned against each other so that the overlap of the pharmacophoric elements responsible for producing a biological response is maximized. In cases where the ligands are very diverse in structure or have several possible modes of binding, developing the alignment can be problematic.

In cases where the crystal structure of the target protein complexed to a ligand has been resolved, the structure of the docked ligand can be used as a template. However, even in this advantageous case it is difficult to deal with compounds in the training set which might have multiple protein binding conformations while maintaining a high pharmacophoric overlap with the template compound. A new approach to this problem is to use a docking program capable of predicting the most favorable conformation of the bound ligand without introducing any human bias. In this study we have utilized the program Gold which has been used extensively to study the docking of ligands in proteins [18–20].

Once a viable docked pose for a given ligand is obtained it is possible to calculate the theoretical binding affinity of the ligands through molecular mechanics calculations. It has been reported by several authors that in many protein–ligand systems there exists a strong correlation between the calculated gas-phase binding affinity and the biological activity of the ligand [21–23]. This type of calculation is feasible for relatively small sets of ligands as calculating these values are quite computationally expensive due to the size of the systems being examined. In a recent publication it has been shown that it is possible to add these calculated binding affinities to CoMFA models in order to improve the predictive nature of the models [24]. We report the use of such an approach in developing predictive models for both the ER $\alpha$  and ER $\beta$  isoforms of the estrogen receptor.

## 2. Methods

### 2.1. Preparation of protein structures

The crystal structure of ER $\alpha$  in complexation with 17 $\beta$ -estradiol (1ERE) [25] and ER $\beta$  in complexation with genistein (1QKM) [26] were extracted from the Research Collaboratory for Structural Bioinformatics Protein Data Bank (RCSB-PDB). These structures were read in and manipulated with the program Maestro [27]. In each case residues in the crystal structure which were missing atoms or missing all together because they could not be experimentally resolved were added in order to complete the protein chain. Hydrogen atoms were assigned to these crystal structures since the X-ray crystallography technique can not resolve the position of these atoms. For each protein–ligand structure the hydrogen atoms were then minimized using the OPLS force field and the corresponding partial-charge description while the rest of the structure was held fixed until the maximum derivative was <0.01 kcal/(mol Å) [28]. The residues which were not resolved in the crystal structure but

complete the protein chain were then minimized until the maximum derivative was  $<0.01$  kcal/(mol Å) while all other atoms were fixed. Finally, for each protein–ligand the entire system was allowed to relax until the maximum derivative was  $<0.01$  kcal/(mol Å), with the exception of the ligand and a single water molecule which is present in both protein–ligand complexes and is considered important for binding [25,26].

## 2.2. Preparation of ligand structures

The A-ring from the crystal structure of  $17\beta$ -estradiol in complexation with  $ER\alpha$  was used as a building block for the construction of molecular models of the other ligands. The ligands were then minimized using the OPLS force field and the corresponding partial-charge description until the maximum derivative was  $<0.001$  kcal/(mol Å). The lowest energy conformation of each ligand was then located by using the Monte Carlo stochastic dynamics (MCM) conformational search routine implemented in MacroModel (Version 8.0) [29]. In each case all rotatable bonds were selected, 50 000 conformations were generated and unique conformations within 2 kcal/mol of the lowest energy conformation were retained.

## 2.3. Docking and calculation of binding energy

The program Gold was used to dock the ligands in the ligand-binding domain (LBD) of both  $ER\alpha$  and  $ER\beta$  respectively [18]. A 16 Å cavity was defined around the carbon atom of the terminal methyl group of residue MET421 in the preprocessed crystal structure of  $ER\alpha$  in complexation with  $17\beta$ -estradiol. In the case of  $ER\beta$  a 16 Å cavity was defined around carbon number 4 of the phenyl ring in residue PHE356 in the preprocessed crystal structure of  $ER\beta$  in complexation with genistein.

Having produced viable poses of the ligands bound to each of the estrogen receptor isoforms with Gold, we proceeded to calculate their theoretical binding affinity by utilizing the EMBRACE procedure developed by Schrödinger Inc. as part of the MacroModel package [29]. The ligands, in their docked conformations, were then submitted to EMBRACE calculations, using the interaction energy mode which we found to be the most predictive method. The binding energy of the ligand can be described as

$$\Delta E = E_{VDW(\text{complex})} + E_{\text{electrostatic}(\text{complex})} \\ + \Delta E[E_{\text{ligand bound}} - E_{\text{ligand unbound}}]$$

where  $E_{VDW}$  refers to the van der Waals steric interaction energy of the protein–ligand complex and  $E_{\text{electrostatic}}$  refers to the corresponding electrostatic interaction energy. Each of the energy terms in the above equation were calculated in the gas-phase and in an implicit aqueous phase using the generalized born surface area (GB/SA) model [30].

## 2.4. CoMFA models

CoMFA models were constructed by extracting the ligands from the minimized protein–ligand complexes and aligning their A-ring mimics to the corresponding A-ring of in the case of our  $ER\alpha$  CoMFA model,  $17\beta$ -estradiol from 1ERE and in the case of our  $ER\beta$  model, genistein from 1QKM. Once the compounds were aligned the electrostatic and steric fields of all of the ligands were calculated by the CoMFA technique. In addition to the standard steric and electrostatic fields calculated in CoMFA our OPLS derived  $NB_{(aq)}$  interaction energies were added to the correlation models to investigate whether their inclusion would aid the predictive nature of our models. Table 3 summarizes the results from a PLS analysis, utilizing the leave-one-out method, of our CoMFA models for all 30 ligands. The value  $q^2$  is a measure of the external predictive nature of the CoMFA model, a  $q^2$  greater than 0.50 said to represent a predictive model of use to the drug design process.

## 3. Results and discussion

Fig. 1 illustrates the chemical structures of the different classes of ER ligands used in this study with their pharmacophoric elements highlighted. An examination of these structures show that virtually all ligands designed to date incorporate at least an A-ring mimic. From the crystal structure 1ERE, the natural estrogen  $17\beta$ -estradiol interacts with  $ER\alpha$  via a hydrogen-bonding network formed from the hydroxy group of the A-ring interacting with ARG394, GLU353 and a single water molecule. The hydroxy group of the D-ring forms a hydrogen bond with HIS524. These hydrogen-bonding interactions form the basis of the favorable binding interaction of  $17\beta$ -estradiol with  $ER\alpha$  and thus are the core elements for a pharmacophoric model of the  $ER\alpha$  binding pocket.

In the case of  $ER\beta$  (1QKM), the ligand genistein interacts in a similar fashion. Genistein interacts with  $ER\beta$  via a hydrogen-bonding network formed by the hydroxy group of the B-ring interacting with ARG346, GLU305 and a single water molecule while the hydroxy group of the A-ring of genistein forms a hydrogen bond with HIS475. As with  $ER\alpha$ , these hydrogen bonding interactions form core elements for a pharmacophoric model of the  $ER\beta$  binding pocket. Tables 1 and 2 list the experimental binding affinity of each of the ligands relative to that of the natural estrogen  $17\beta$ -estradiol which is arbitrarily set at 100. Given the relative binding affinity (RBA) in both  $ER\alpha$  and  $ER\beta$  it is simple to evaluate the ER subtype selectivity of the ligands also listed in the tables.

As one can see from Table 1 diethylstilbestrol exhibits the highest RBA for  $ER\alpha$  while from Table 2 the novel non-steroidal compound trans-5,11-diethyl-5,6,11,12-tetrahydrochrysene-2,8-diol exhibits the highest RBA for  $ER\beta$ . However, neither of these ligands exhibit high specificity for

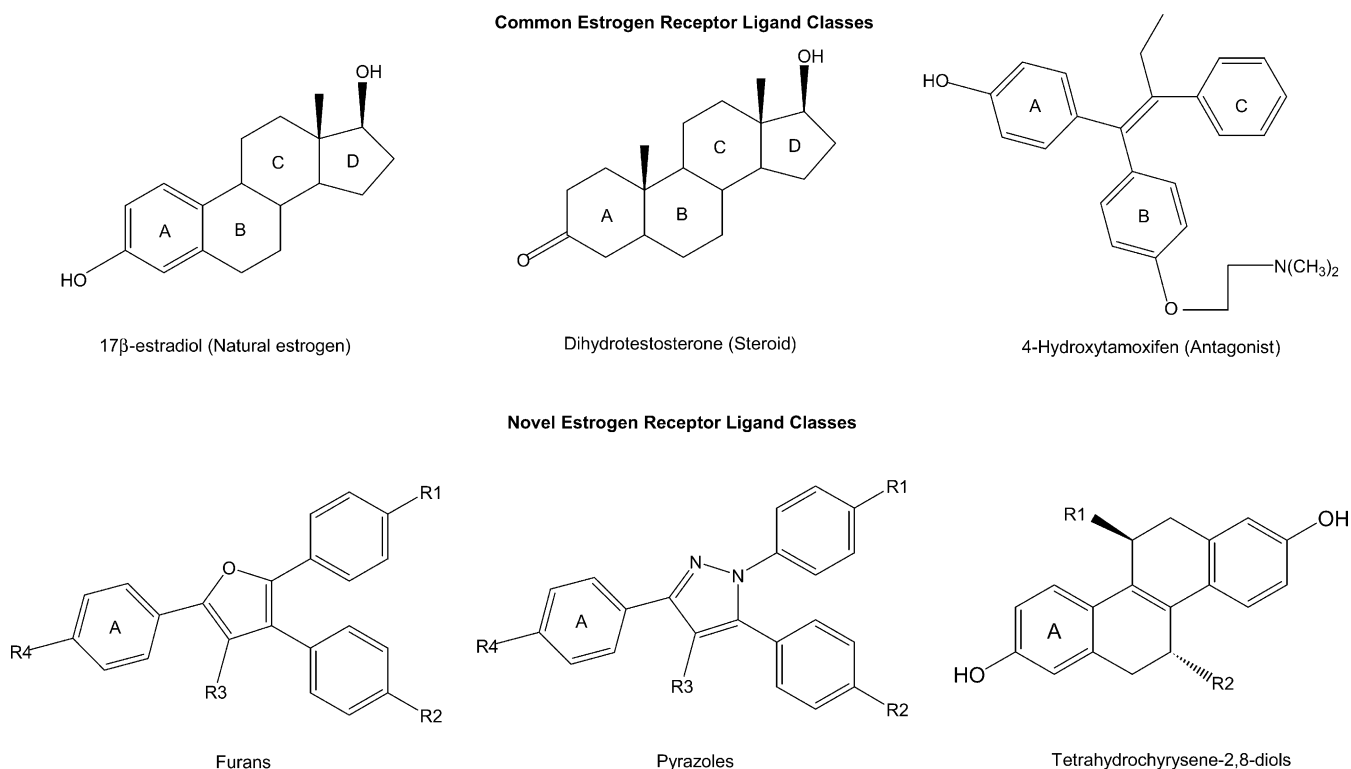


Fig. 1. Estrogen receptor ligand classes used in this study with their pharmacophoric elements highlighted.

either ER $\alpha$  or ER $\beta$  having a RBA ratio (ER $\alpha$ /ER $\beta$ ) of 1.6 and 0.5, respectively. As a result it is difficult to extrapolate whether the observed biologic responses are due to a preferential interaction with one particular isoform. However, as one can see from Table 2 the novel non-steroidal substituted furans and pyrazoles exhibit unprecedented estrogen subtype selectivity compared to the classical ER ligands listed in Table 1. In particular the compound 4-propyl-1,3,5-triphenolpyrazole (PPT) has been reported to have a 400-fold affinity for the ER $\alpha$  isoform. It is essential to note that the origin of this enhanced specificity for ER $\alpha$

comes from the ligands poor affinity to bind in ER $\beta$  (Table 2, RBA ER $\beta$  0.12). Understanding the origin of the biological discrimination of PPT in ER $\beta$  is of great importance since it might be lead to the development of more potent selective ER ligands.

The program Gold was used to dock the ligands in the ligand-binding domain of both ER $\alpha$  and ER $\beta$ , respectively [18]. The result from a Gold run is a series of viable conformations of the ligand docked inside the LBD of the target protein together with an associated fitness function and other measures of the corresponding protein–ligand interaction energy. As a validation of the accuracy of the docking program Gold and approach used in this study the root-mean squared (r.m.s.) deviation of the crystal structure of 17β-estradiol from 1ERE was compared against the most favorably ranked conformation of 17β-estradiol docked with Gold. Likewise the r.m.s. of the crystal structure of genistein from 1QKM was compared with the Gold docked genistein. The r.m.s. deviation between the experimental docked conformation and the calculated docked conformation for 17β-estradiol in ER $\alpha$  was 0.26 and 0.39 for genistein in ER $\beta$ . Given the low r.m.s. deviation between the experimental structures and the calculated docked structures it is reasonable to expect that the program would exhibit a similar accuracy with the other ligands utilized in the study. Indeed Gold was able to locate viable docking conformations, i.e. inside the LBD, of all of the ligands presented to it.

One surprising outcome from the docking study was that Gold found essentially a flipped conformation, relative to the

Table 1  
Experimental relative binding affinities of common estrogenic ligands

Ligand	RBA <sup>a</sup>		Ratio RBA (ER $\alpha$ /ER $\beta$ )
	ER $\alpha$	ER $\beta$	
17β-Estradiol	100	100	1
17α-Estradiol	58	11	5.3
Genistein	5	36	0.1
Diethylstilbestrol	468	295	1.6
Dienestrol	223	404	0.6
4-OH-tamoxifen	178	339	0.5
Tamoxifen	7	6	1.2
Methoxychlor	0.01	0.13	0.1
5-Androstenediol	6	17	0.4
Dihydrotestosterone	0.05	0.17	0.3
Norethindrone	0.07	0.01	7
Testosterone	<0.01	<0.01	1

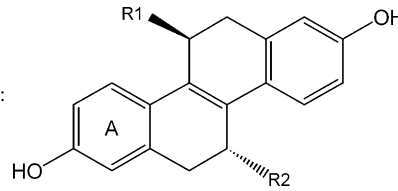
<sup>a</sup> Determined by competitive radiometric binding assay, where the RBA of 17β-estradiol is arbitrarily set at 100.

Table 2  
Experimental relative binding affinities of novel estrogenic ligands

Ligand/ID	R-groups				RBA <sup>a</sup>		$\alpha/\beta$
	R1	R2	R3	R4	ER $\alpha$	ER $\beta$	

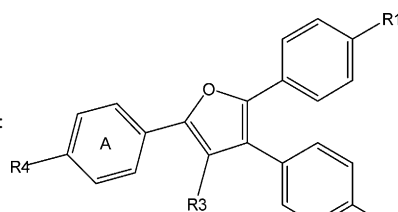
Tetrahydrochrysene-2,8-diols:



<b>1a</b>	(R)Me	(S)Me			222 ± 18	254 ± 57	1
<b>1b</b>	(R)Et	(S)Et			221 ± 42	432 ± 21	0.5
<b>1c</b>	(R)Pr	(S)Pr			33.6 ± 2.8	92.3 ± 4.5	0.4
<b>1d</b>	(S)Pr	(S)Pr			1.6 ± 0.4	5.1 ± 4.0	0.3

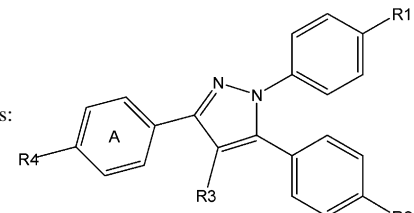
Furans:



<b>1e</b>	OH	OH	Et	OH	140 ± 38	2.9 ± 0.1	48
<b>1f</b>	OH	OH	Pr	OH	100 ± 14	1.8 ± 0.65	56
<b>1g</b>	H	OH	Et	OH	82 ± 20	7.1 ± 1.2	12
<b>1h</b>	H	OH	Pr	OH	140 ± 13	15 ± 4.1	9.5
<b>1i</b>	H	H	Et	OH	10.8 ± 2.6	3.4 ± 1.2	3.8
<b>1j</b>	H	OH	Et	H	0.15 ± 0.01	0.07 ± 0.02	2.1

Pyrazoles:



<b>1k</b>	H	OH	Et	OH	31 ± 0.15	1.1 ± 0.2	28
<b>1l</b>	H	OH	Pr	OH	16.8 ± 0.3	0.52 ± 0.03	32
<b>1m</b>	H	OH	<i>i</i> -Bu	OH	56 ± 6	1.4 ± 0	40
<b>1n</b>	H	OH	Bu	OH	8.7 ± 2.0	0.47 ± 0.1	19
<b>1o</b>	OH	OH	Pr	OH	49 ± 12	0.12 ± 0.04	410
<b>1p</b>	OH	OH	<i>i</i> -Bu	OH	75 ± 6	0.89 ± 0.06	84
<b>1q</b>	H	OH	<i>i</i> -Pr	OH	5.6 ± 2	0.86 ± 0.11	6.5
<b>1r</b>	H	OH	Et	H	0.04 ± 0.11	0.06 ± 0.01	0.7

<sup>a</sup> Determined by competitive radiometric binding assay, where the RBA of 17 $\beta$ -estradiol is arbitrarily set at 100. Values represent the average ( $\pm$ S.D. or range) of multiple determinations.

same docked ligand in ER $\alpha$ , for the substituted furans and pyrazoles in ER $\beta$ . Fig. 2 illustrates the most favorable docking conformation for the ligand PPT, the most ER subtype selective ligand, in the LBD of ER $\alpha$  and ER $\beta$ . Upon further analysis it appears that residue PHE356 in ER $\beta$  which is identical to residue PHE404 in ER $\alpha$  protrudes into the  $\alpha$ -face of the cavity of the LBD to a much greater extent in ER $\beta$  than in ER $\alpha$ . As a result if the ligands were bound in the same conformation in ER $\alpha$  and ER $\beta$ , illustrated in Fig. 2b, the functional groups added to the substituted furans/pyrazoles, which are considered to be the origin of the specificity of these ligands for ER $\alpha$  over ER $\beta$ , would be in too close contact with residue PHE356. Furthermore, from

Fig. 2 the *n*-propyl group of PPT interacts with residues in the  $\beta$ -face of the cavity of the ER $\beta$  LBD, particularly TRP335 and MET336, and with residues in the  $\alpha$ -face of the cavity of the ER $\alpha$  LBD, particularly PHE404 and MET421. This is an important finding since it suggests if true that the origin of the specificity of these novel compounds comes from this alternative docking conformation in ER $\beta$  relative to ER $\alpha$ . Obviously if residues in the LBD of ER $\alpha$  are simply mutated to represent the LBD of ER $\beta$  this configuration would not be observed since PHE404 in its ER $\alpha$  conformation would simply become PHE356. Of course it is possible that PHE356 could adopt an alternate conformation in ER $\beta$  to accommodate PPT and ligands like it in the  $\alpha$ -



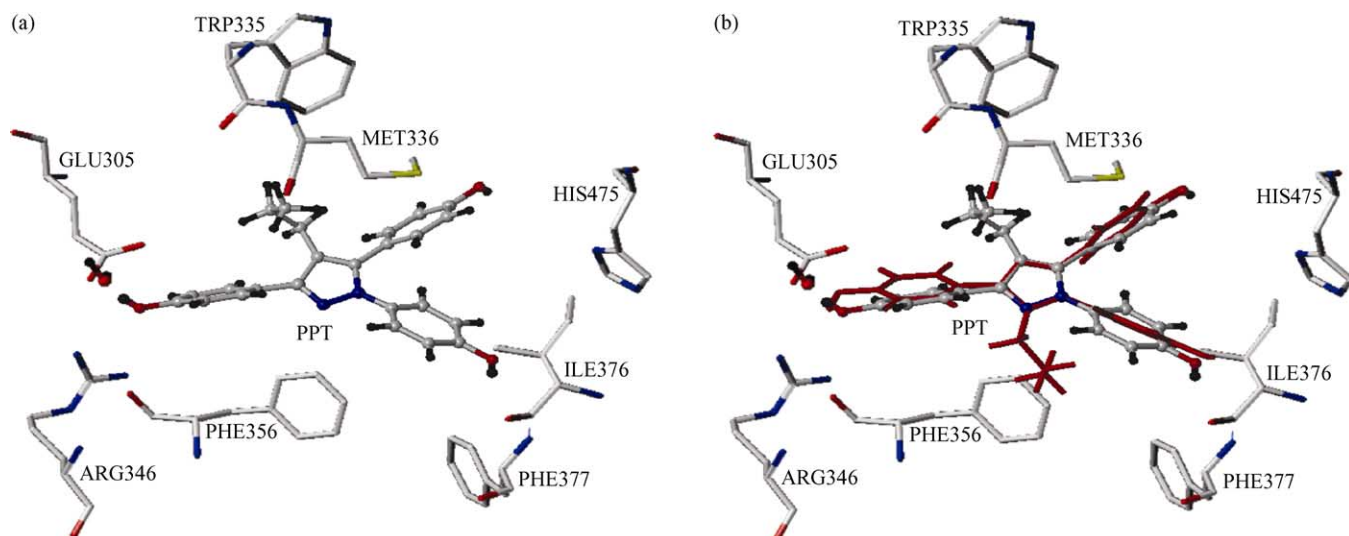


Fig. 2. Unbiased best fit configuration of 4-propyl-1,3,5-triphenolpyrazole (PPT) in (a) ER $\alpha$  and (b) ER $\beta$ , the predicted conformation of PPT in ER $\alpha$  is overlaid in red in order to highlight the flipped conformation.

face of the cavity of the LBD however our theoretical studies do not suggest this to be the case as will be discussed below.

Looking closer at the docked poses produced by Gold, Fig. 3 is an illustration of the hydrogen bonding network observed in our final minimized models of PPT in ER $\alpha$  and ER $\beta$  utilizing the program LIGPLOT [31]. Generally the

significant hydrogen bonding network described earlier, between the A-ring mimic of the ligand and the GLU, ARG, HIS residues and conserved water in the corresponding ER, are observed. From Fig. 3 it can be seen that differences in the magnitudes of these hydrogen bonds are subtle for PPT in ER $\alpha$  and ER $\beta$ . For example the hydrogen bond distances

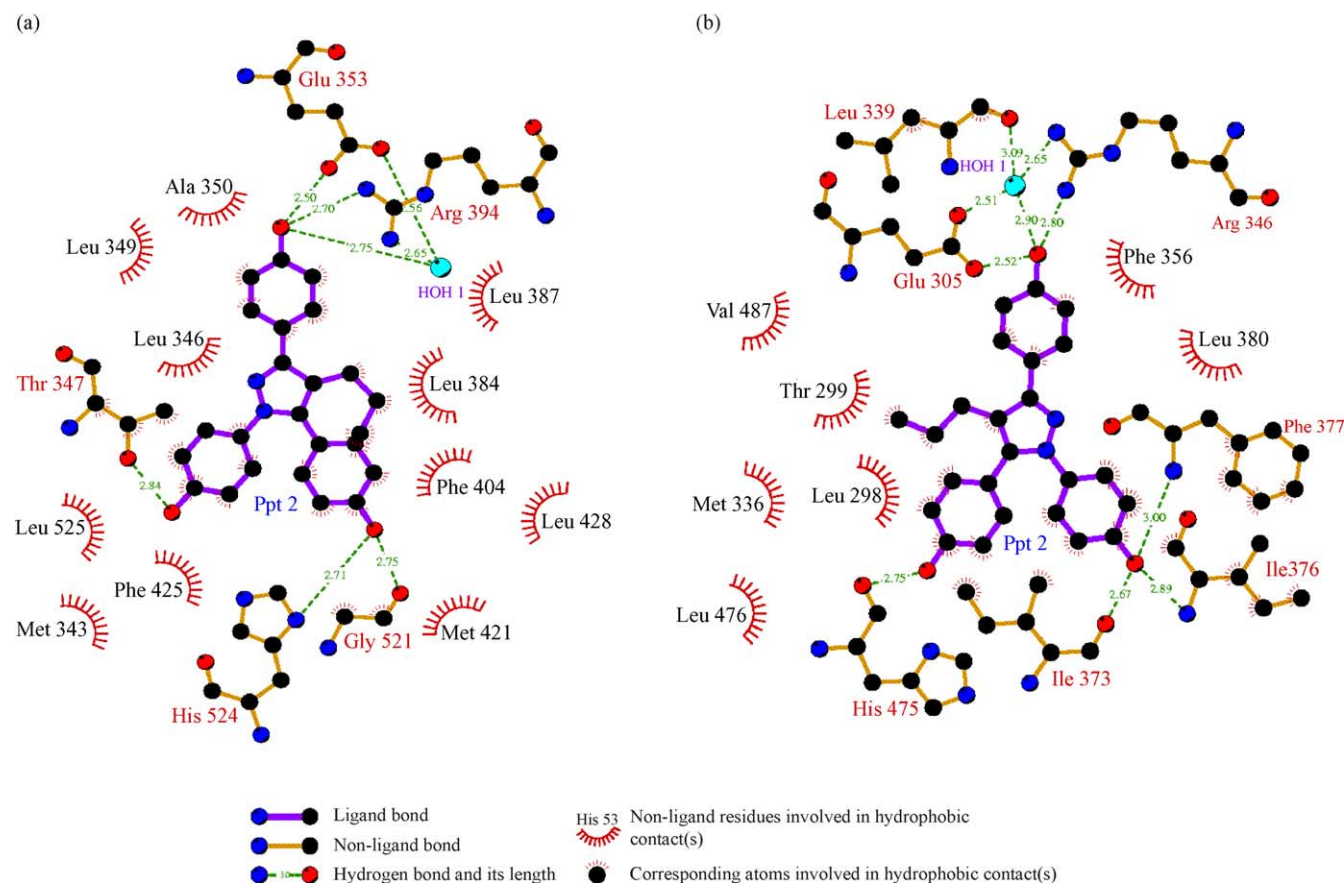


Fig. 3. Schematic of H-Bonding network of PPT minimized in (a) ER $\alpha$  and (b) ER $\beta$  generated using LIGPLOT.

between the heavy atoms of the R2 phenol group of PPT and the HIS group of the corresponding protein are 2.75 and 2.71 Å, respectively. Of greater interest are the corresponding interactions of the *n*-propyl group of PPT in ER $\alpha$  and ER $\beta$ . As discussed in the docking section, in ER $\alpha$  we find that the propyl group interacts with residues in the  $\alpha$ -face of the cavity of the ER $\alpha$  LBD, particularly PHE404 and MET421. While in ER $\beta$  the normal propyl group of PPT interacts with residues in the  $\beta$ -face of the cavity of the ER $\beta$  LBD, particularly TRP335 and MET336, because of its flipped orientation. Furthermore, this flipped orientation is due to the proximity of PHE356 in ER $\beta$ , even after minimization, PHE356 being equivalent to PHE404 in ER $\alpha$  that does not protrude into the  $\alpha$ -face of the ligand-binding domain.

Having produced viable poses of the ligands bound to each of the estrogen receptor isoforms we proceeded to calculate their theoretical binding affinity by utilizing the EMBRACE procedure developed by Schrödinger Inc. as part of the MacroModel package [29]. This procedure has been specifically designed for the calculation of protein–ligand binding energies. The key advantage to this approach is that one needs only one model of the protein target structure used in the docking procedure. The ligands, in their docked conformations, are added to a molecular spreadsheet

and the parameters for the EMBRACE calculation such as the force field to use, dielectric constant and mode of energy calculation are specified. In our research we have found the interaction energy mode to be the most predictive method where the binding energy of the ligand can be described as

$$\Delta E = E_{\text{VDW}(\text{complex})} + E_{\text{electrostatic}(\text{complex})} + \Delta E[E_{\text{ligand bound}} - E_{\text{ligand unbound}}]$$

where  $E_{\text{VDW}}$  refers to the van der Waals steric interaction energy of the protein–ligand complex and  $E_{\text{electrostatic}}$  refers to the corresponding electrostatic interaction energy. Obviously each of the energy terms in the above equation can be calculated in the gas-phase or in an aqueous-phase using the generalized born surface area model [30].

Table 3 summarizes the results from a partial-least squares analysis (PLS) of the predictive nature of the calculated interaction energies for all protein–ligand complexes in both ER $\alpha$  and ER $\beta$ , utilizing the leave-one-out method. From Table 3 the non-bonded (NB) interactions calculated in the gas-phase were found to be the most predictive indicator of biological activity which is in agreement with the work of Pérez et al. [23]. Inclusion of solvation energies and the energy difference between the

Table 3  
Results from various PLS models for ER $\alpha$  and ER $\beta$

PLS model	$r^2$	$q^2$	S.E.E.	$F$	PC	$n$
ER $\alpha$						
Binding energy and non-bonded interactions						
NB <sub>(g)</sub>	0.65	0.60	0.84	51	1	30
$\Delta E_{(g)}$	0.58	0.51	0.92	38	1	30
NB <sub>(aq)</sub>	0.37	0.30	1.12	16	1	30
$\Delta E_{(aq)}$	0.50	0.42	1.00	28	1	30
Individual classes						
Estrogen, NB <sub>(g)</sub>	0.67	0.57	0.97	28	1	16
Furan/pyrazole, NB <sub>(g)</sub>	0.74	0.63	0.57	34	1	14
CoMFA						
log RBA vs. CoMFA	0.99	0.67	0.13	558	6	30
log RBA vs. CoMFA + NB <sub>(g)</sub>	0.99	0.73	0.17	323	6	30
ER $\beta$						
Binding energy and non-bonded interactions						
NB <sub>(g)</sub>	0.42	0.35	1.06	20	1	30
$\Delta E_{(g)}$	0.41	0.34	1.07	19	1	30
NB <sub>(aq)</sub>	0.23	0.12	1.22	8	1	30
$\Delta E_{(aq)}$	0.24	−0.12	1.21	9	1	30
Individual classes						
Estrogen, $\Delta E_{(aq)}$	0.81	0.75	0.72	60	1	16
Furan/pyrazole, NB <sub>(g)</sub>	0.63	0.52	0.45	21	1	14
CoMFA						
log RBA vs. CoMFA	0.99	0.66	0.18	267	6	30
log RBA vs. CoMFA + NB <sub>(g)</sub>	0.99	0.74	0.18	280	6	30

$r^2$  refers to non-validated correlation,  $q^2$  to the cross-validated correlation,  $F$  is a measure of the statistical significance of the model, S.E.E. refers to the standard error of estimate, NB refers to OPLS derived non-bonded interactions,  $\Delta E$  refers to the OPLS derived binding energy and the corresponding subscripts, (g) and (aq), refer to whether the energy was calculated in the gas-phase or in aqueous solution.

Table 4

Extraction of test-set and recalculation of most predictive PLS models

PLS model	$r^2$	$q^2$	S.E.E.	$F$	PC	$n$
<b>ER<math>\alpha</math></b>						
Ia (log RBA vs. CoMFA)	0.99	0.57	0.13	431	6	24
IIa (log RBA vs. CoMFA + NB <sub>(g)</sub> )	0.99	0.67	0.14	374	2	24
IIIa (NB <sub>(g)</sub> )	0.64	0.57	0.87	37	1	24
IVa (Estrogen, NB <sub>(g)</sub> )	0.63	0.50	1.05	19	1	13
IVa (Furan/pyrazole, NB <sub>(g)</sub> )	0.78	0.69	0.56	32	1	11
<b>ER<math>\beta</math></b>						
Ib (log RBA vs. CoMFA)	1.00	0.68	0.05	3185	6	24
IIb (log RBA vs. CoMFA + NB <sub>(g)</sub> )	1.00	0.73	0.04	5553	6	24
IIIb (NB <sub>(g)</sub> )	0.42	0.34	1.11	16	1	24
IVb (Estrogen, $\Delta E_{(aq)}$ )	0.82	0.74	0.74	50	1	13
IVb (Furan/pyrazole, NB <sub>(g)</sub> )	0.57	0.41	0.48	12	1	11

$r^2$  refers to non-validated correlation,  $q^2$  to the cross-validated correlation,  $F$  is a measure of the statistical significance of the model, S.E.E. refers to the standard error of estimate, NB refers to OPLS derived non-bonded interactions,  $\Delta E$  refers to the OPLS derived binding energy and the corresponding subscripts, (g) and (aq), refer to whether the energy was calculated in the gas-phase or in aqueous solution.

ligand in its bound and free states did little to enhance the correlation to the biological response. A cross-validated  $r^2(q^2) > 0.50$  is generally considered the measure that the corresponding model is predictive and of use to the drug design process hence our ER $\alpha$  NB<sub>(g)</sub> model is predictive,  $q^2 = 0.60$  and the standard error of estimate (S.E.E.) = 0.84. However, the corresponding values for ER $\beta$  are poorer,  $q^2 = 0.35$  and S.E.E. = 1.06, hence not predictive. We investigated the origin of this poor performance of our ER $\beta$  models further by dividing the ligands into two distinct classes, those that resembled a steroid and those that were based on a substituted furan or pyrazole. The PLS models were regenerated and it was found that the correlation's were significantly better in the case of our ER $\beta$  models but not our ER $\alpha$  models. In particular we found that our calculated aqueous-phase binding energy model  $\Delta E_{(aq)}$  was significantly more predictive for the estrogen set in ER $\beta$ ,  $q^2 = 0.75$  and S.E.E. = 0.72. While the furan–pyrazole ER $\beta$  model also became predictive with a  $q^2 = 0.52$  and S.E.E. = 0.45. We attribute the change in significance and predictive ability of these individual ER $\beta$  models to the fact that the furan–pyrazole ER $\beta$  set generally exhibit poor biological activity hence the experimental data is skewed towards low binding (Table 2) with the result being that the predicted furan–pyrazole biological data does not fit the predicted estrogen biological data.

From the CoMFA results shown in Table 3 it can be seen that in each case a strong correlation can be found between the calculated CoMFA molecular interaction fields and the observed relative binding affinity, ER $\alpha$ :  $r^2 = 0.99$ ,  $q^2 = 0.67$ , S.E.E. = 0.13 and  $F = 558$ , ER $\beta$ :  $r^2 = 0.99$ ,  $q^2 = 0.66$ , S.E.E. = 0.18 and  $F = 267$ . While inclusion of the OPLS derived NB<sub>(aq)</sub> interaction energies does improve the external predictive nature of both models ER $\alpha$ :  $q^2 = 0.73$  and ER $\beta$ :  $q^2 = 0.74$ . At this point in order to validate and test the predictive power of all our derived models we re-scrambled our ligands and extracted six at random to act as a test-set leaving 24 ligands to reconstruct the PLS models.

The six extracted ligands were, **1p**, **1f**, **1h**, 17 $\alpha$ -estradiol, 4-hydroxytamoxifen and dihydrotestosterone (DHT). Table 4 summarizes the results from the PLS analysis of the models reconstructed from the most predictive models in Table 3. While Table 5 tabulates the predicted log<sub>10</sub> RBA and corresponding residuals, difference between predicted and experiment, for all ligands using the two CoMFA models in Table 4. It can be seen that the correlation predictors,  $r^2$ ,  $q^2$ , etc., for the training-set of 24 ligands (Table 4), behave consistently with the corresponding results in Table 3 despite the number of ligands falling. This suggests that the models are robust and that the predictive power is independent of number of ligands in the training-set. For example the ER $\beta$  CoMFA only model with all thirty ligands exhibits a  $r^2 = 0.99$  and  $q^2 = 0.66$  while that of the training-set exhibits a  $r^2 = 1.00$  and  $q^2 = 0.68$ . In terms of the test-set the average residual using the CoMFA model to predict the biological activity of the test-set ligands in both ER $\alpha$  and ER $\beta$  is 0.52 (models Ia and Ib) while as the  $q^2$  suggests addition of the OPLS derived NB<sub>(aq)</sub> interaction energies does improve the external predictive nature of both models with an average residual of 0.38 (models IIa and IIb). Of the six ligands in the test-set, regardless of which PLS model is used, the activity of DHT is consistently poorly predicted particularly in the ER $\beta$  models suggesting maybe a poor alignment of this ligand in the ER $\beta$  model.

Fig. 4 illustrates the standard deviation of the calculated three-dimensional molecular fields from our most predictive ER $\alpha$  and ER $\beta$  CoMFA models (Table 4). Within these molecular fields the ligand PPT has been superimposed in the same orientation for easy comparison. In each case contours of the steric map are shown in yellow and green, while those of the electrostatic map are shown in red and blue. Increased biological activity is correlated with: more bulk near green; less bulk near yellow; more positive charge near blue, and more negative charge near red. As a result these fields could be manipulated in order to increase the subtype selectivity of ligand PPT. For example, one might



Table 5  
Predicted activities using PLS models (I) and (II)

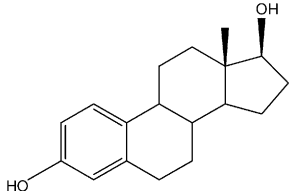
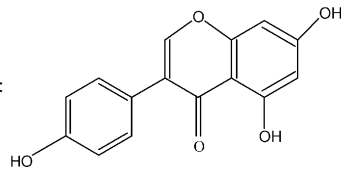
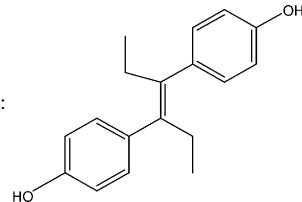
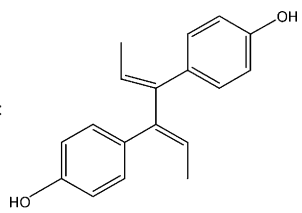
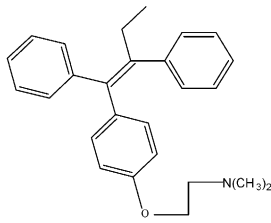
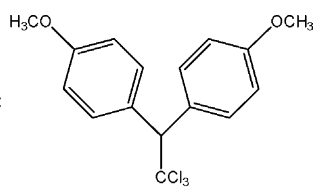
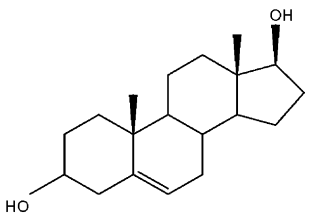
Ligand	$\log_{10}$ RBA ER $\alpha$					$\log_{10}$ RBA ER $\beta$				
	Exp.	Model Ia		Model IIa		Exp.	Model Ib		Model IIb	
		Pred.	$\delta$	Pred.	$\delta$		Pred.	$\delta$	Pred.	$\delta$
17 $\beta$ -Estradiol: 	2.00	2.07	−0.07	1.97	0.03	2.00	2.00	0.00	1.93	0.07
Genistein: 	0.70	0.71	−0.01	0.67	0.03	1.56	1.53	0.03	1.55	0.01
Diethylstilbestrol: 	2.67	2.68	−0.01	2.77	−0.10	2.47	2.43	0.04	2.44	0.03
Dienestrol: 	2.35	2.32	0.03	2.39	−0.04	2.61	2.60	0.01	2.62	−0.01
Tamoxifen: 	0.85	0.97	−0.12	1.02	−0.17	0.78	0.79	−0.01	0.82	−0.04
Methoxychlor: 	−2.00	−1.95	−0.05	−2.06	0.06	−0.89	−0.86	−0.03	−0.91	0.02
5-Androstenediol: 	0.78	0.71	0.07	0.91	−0.13	1.23	1.24	−0.01	1.29	−0.06

Table 5 (Continued)

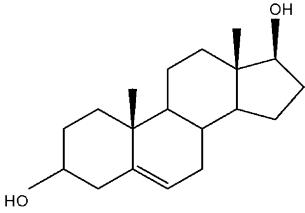
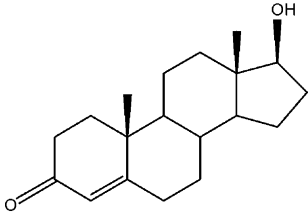
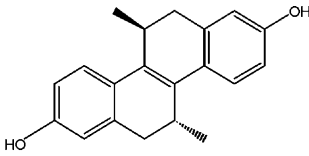
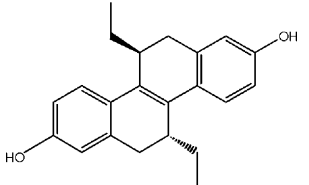
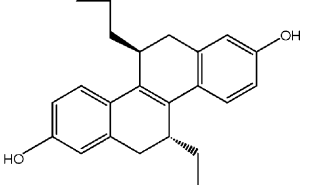
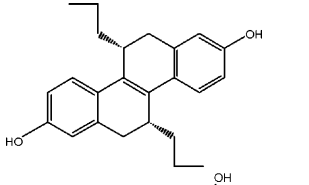
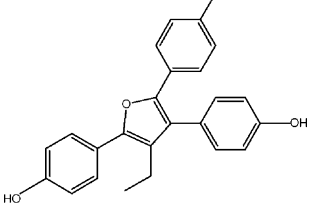
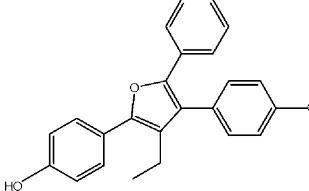
Ligand	$\log_{10}$ RBA ER $\alpha$					$\log_{10}$ RBA ER $\beta$				
	Exp.	Model Ia		Model IIa		Exp.	Model Ib		Model IIb	
		Pred.	$\delta$	Pred.	$\delta$		Pred.	$\delta$	Pred.	$\delta$
Norethindrone: 	−1.15	−1.43	0.28	−1.22	0.07	−2.00	−2.13	0.13	−2.01	0.01
Testosterone: 	−2.00	−1.79	−0.21	−1.88	−0.12	−2.00	−1.88	−0.12	−1.99	−0.01
1a: 	2.35	2.29	0.06	2.22	0.13	2.40	2.41	−0.01	2.38	0.02
1b: 	2.34	2.16	0.18	2.15	0.19	2.64	2.66	−0.02	2.69	−0.05
1c: 	1.53	1.71	−0.18	1.84	−0.31	1.97	1.98	−0.01	1.95	0.02
1d: 	0.20	0.04	0.16	0.03	0.17	0.71	0.68	0.03	0.71	0.00
1e: 	2.15	2.18	−0.03	2.02	0.13	0.46	0.49	−0.03	0.48	−0.02
1g: 	1.91	1.96	−0.05	1.90	0.01	0.85	0.88	−0.03	0.86	−0.01

Table 5 (Continued)

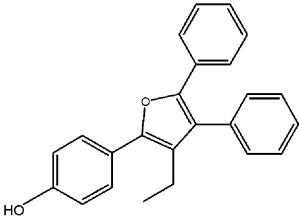
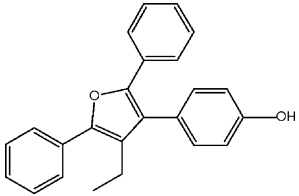
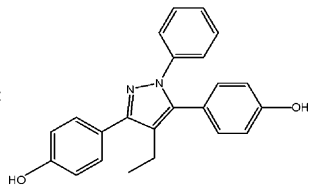
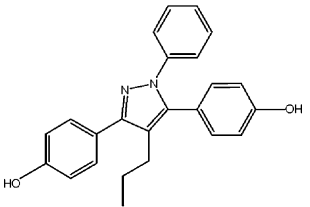
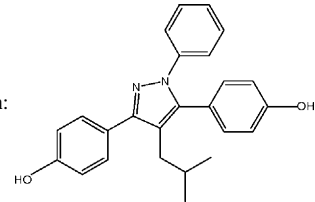
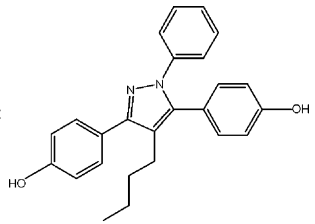
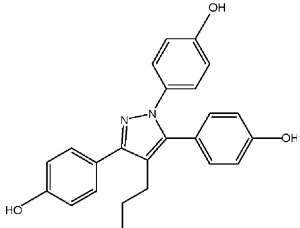
Ligand	log <sub>10</sub> RBA ER $\alpha$					log <sub>10</sub> RBA ER $\beta$				
	Exp.	Model Ia		Model IIa		Exp.	Model Ib		Model IIb	
		Pred.	$\delta$	Pred.	$\delta$		Pred.	$\delta$	Pred.	$\delta$
<b>1i:</b> 	1.03	0.96	0.07	0.94	0.09	0.53	0.57	−0.04	0.49	0.04
<b>1j:</b> 	−0.80	−0.81	0.01	−0.74	−0.06	−1.15	−1.16	0.01	−1.20	0.05
<b>1k:</b> 	1.49	1.44	0.05	1.52	−0.03	0.04	0.02	0.02	0.07	−0.03
<b>1l:</b> 	1.23	1.17	0.06	1.29	−0.06	−0.28	−0.27	−0.01	−0.25	−0.03
<b>1m:</b> 	1.75	1.83	−0.08	1.77	−0.02	0.15	0.13	0.02	0.12	0.03
<b>1n:</b> 	0.94	0.95	−0.01	0.73	0.21	−0.33	−0.35	0.02	−0.31	−0.02
<b>1o (PPT):</b> 	1.69	1.64	0.05	1.72	−0.03	−0.92	−0.93	0.01	−0.93	0.01

Table 5 (Continued)

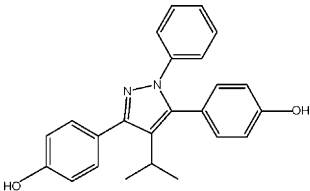
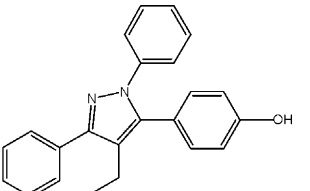
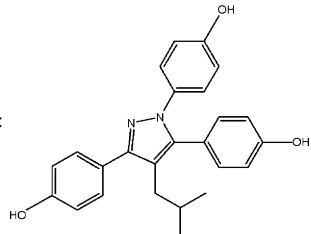
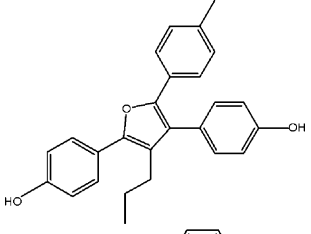
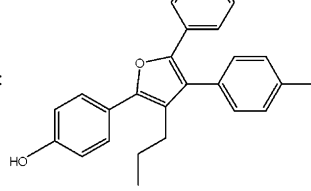
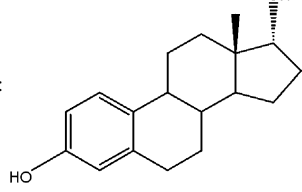
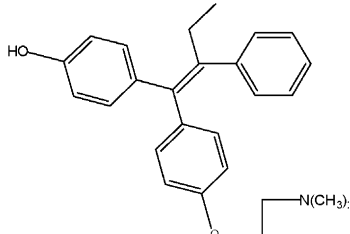
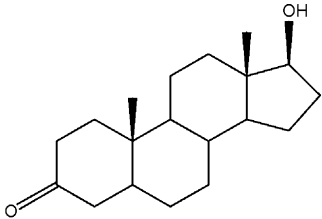
Ligand	$\log_{10}$ RBA ER $\alpha$					$\log_{10}$ RBA ER $\beta$				
	Exp.	Model Ia		Model IIa		Exp.	Model Ib		Model IIb	
		Pred.	$\delta$	Pred.	$\delta$		Pred.	$\delta$	Pred.	$\delta$
<b>1q:</b> 	0.75	0.91	−0.16	0.72	0.03	−0.07	−0.09	0.02	−0.07	0.00
<b>1r:</b> 	−1.40	−1.35	−0.05	−1.33	−0.07	−1.22	−1.20	−0.02	−1.20	−0.02
Test-set										
<b>1p:</b> 	1.88	1.28	−0.60	2.52	0.64	−0.05	0.56	0.61	0.18	0.23
<b>1f:</b> 	2.00	1.55	−0.45	1.83	−0.17	0.26	0.16	−0.10	0.60	0.44
<b>1h:</b> 	2.15	1.25	−0.90	1.60	−0.55	1.18	0.68	−0.50	1.02	−0.16
<b>17<math>\alpha</math>-Estradiol:</b> 	1.76	1.99	+0.23	1.84	0.08	1.04	1.74	0.70	1.30	0.26
<b>4-Hydroxytamoxifen:</b> 	2.25	2.06	−0.19	2.47	0.22	2.53	1.91	−0.62	2.75	0.22

Table 5 (Continued)

Ligand	log <sub>10</sub> RBA ER $\alpha$					log <sub>10</sub> RBA ER $\beta$				
	Exp.	Model Ia		Model IIa		Exp.	Model Ib		Model IIb	
		Pred.	$\delta$	Pred.	$\delta$		Pred.	$\delta$	Pred.	$\delta$
Dihydrotestosterone:										
	-1.30	-1.37	-0.07	-1.69	-0.39	-0.77	-2.00	-1.23	-1.95	-1.18

Exp. refers to experimental data, Pred. refers to predicted data and  $\delta$  refers to the corresponding residual.

Table 6  
Ability of PLS models to rank ligands in the test-set in terms of their ER selectivity

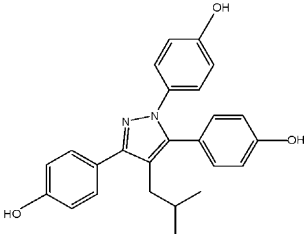
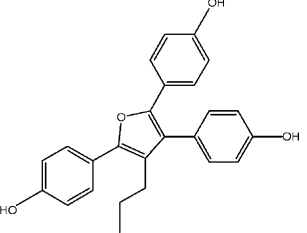
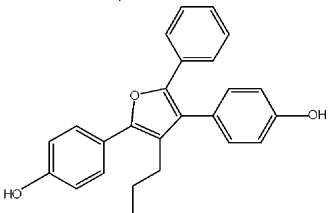
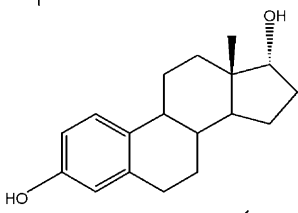
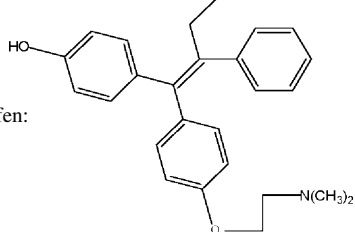
Ligand	Exp.		CoMFA Pred. (Ia, Ib)		$\Delta E$ Pred. (IVa, IVb)		CoMFA + NB <sub>(g)</sub> Pred. (IIa, Iib)	
	$\alpha/\beta$	Rank	$\alpha/\beta$	Rank	$\alpha/\beta$	Rank	$\alpha/\beta$	Rank
<b>1p:</b>								
	84	1	5.2	2	229	1	219	1
<b>1f:</b>								
	56	2	24.5	1	29.5	2	17	2
<b>1h:</b>								
	9.5	3	3.7	4	1.9	4	3.8	3
<b>17<math>\alpha</math>-Estradiol:</b>								
	5.3	4	1.8	5	1.4	5	3.5	4
<b>4-Hydroxytamoxifen:</b>								
	0.5	5	1.4	6	<0.01	6	0.5	6



Table 6 (Continued)

Ligand	Exp.		CoMFA Pred. (Ia, Ib)		$\Delta E$ Pred. (IVa, IVb)		CoMFA + NB <sub>(g)</sub> Pred. (IIa, IIb)	
	$\alpha/\beta$	Rank	$\alpha/\beta$	Rank	$\alpha/\beta$	Rank	$\alpha/\beta$	Rank
Dihydrotestosterone:	0.3	6	4.3	3	5.8	3	1.8	5

Exp. refers to experimental data, Pred. refers to predicted data, NB<sub>(g)</sub> refers to OPLS derived gas-phase non-bonded interactions,  $\Delta E$  refers to the OPLS derived binding energy and  $\alpha/\beta$  refers to the ratio of the experimental relative binding affinity in ER $\alpha$  and ER $\beta$  giving the ER selectivity of the ligand.

want to increase the biological activity of PPT in ER $\alpha$  using the ER $\alpha$  molecular fields for guidance. While at the same time decreasing the biological activity of PPT in ER $\beta$ , using in turn the ER $\beta$  molecular fields for guidance.

Finally, one of the principle goals of this study was too develop models that could predict the ER subtype selectivity of novel ligands not included in the study so as to aid the SERM radiopharmaceutical development process. To fulfill

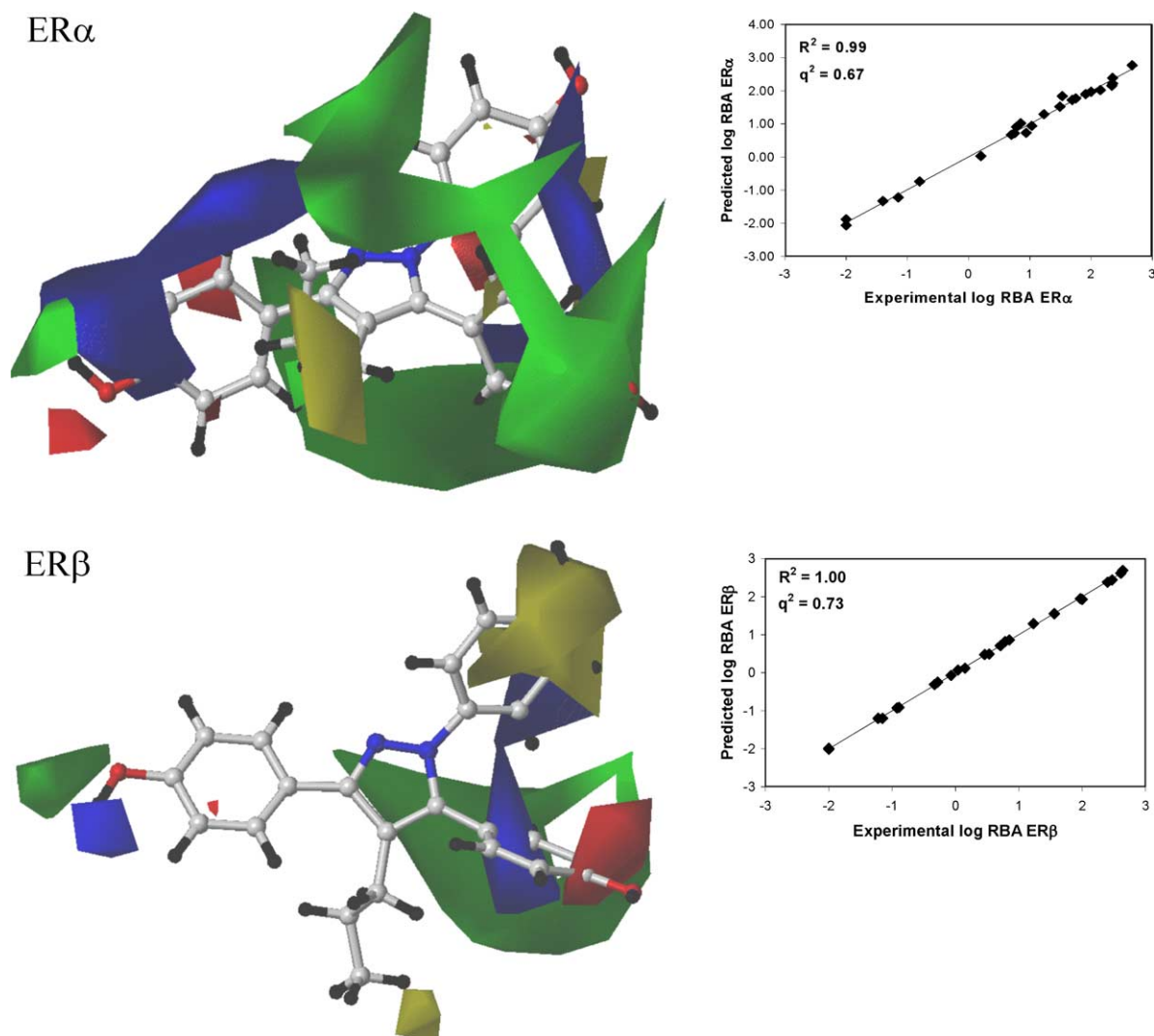


Fig. 4. CoMFA derived molecular field maps with the highly subtype ER selective ligand PPT illustrated. Contours of the steric map are shown in yellow and green, while those of the electrostatic map are shown in red and blue. Increased biological activity is correlated with: more bulk near green; less bulk near yellow; more positive charge near blue, and more negative charge near red.

this goal the ER subtype selectivity of the test-set ligands was predicted using essentially the three distinct predictive models used in this study, OPLS derived energy, CoMFA only and CoMFA plus OPLS derived  $NB_{(g)}$ . Table 6 summarizes the results from this analysis. The performance of each model was evaluated based on their ability to rank these ligands in order of increasing  $RBA(ER\alpha/ER\beta)$ . As one can see although the CoMFA only model (Ia, Ib) ranks **1p** and **1f** ahead of the other four ligands it has them in the wrong order with **1f** being predicted to be more selective than **1p**, while it predicts DHT to be the third most selective ligand. The OPLS derived energy only method (IVa, IVb) performs slightly better given that it ranks **1p** and **1f** correctly but again DHT is poorly predicted. However, the combined model (IIa, IIb) performs best ranking four out of six correctly with only the two least selective ligands 4-hydroxytamoxifen and DHT being incorrectly ranked lending credence to the idea of combining these two techniques in order to develop more predictive models.

#### 4. Conclusions

In conclusion we have utilized the computational techniques of CoMFA, the unbiased docking of ligands utilizing Gold and the fundamental calculation of the binding affinity in order to study the origin of the subtype selectivity of three distinct classes of novel subtype selective estrogen ligands. Our unbiased docking study has highlighted a distinct binding configuration for those novel estrogen ligands based on a pyrazole or furan backbone in  $ER\beta$  which may well prove to be the origin of their enhanced specificity for  $ER\alpha$ . Robust CoMFA models, consisting of several classes of ER ligands, have been developed and validated extensively within the framework of our original set of ligands. Indeed, we have shown how these predictive CoMFA models, particularly when combined with a fundamental measure of non-bonded interactions between the ligands and the protein when bound, that can be used to focus and prescreen new ligands for their ER subtype selectivity prior to experimental determination.

#### Acknowledgement

We wish to thank the National Institute of Biomedical Imaging and Bioengineering, EB00340, for funding this research.

#### References

[1] K.S. Korach, P. Sarver, K. Chae, J.A. McLachlan, J.D. McKinney, Estrogen receptor binding activity of polychlorinated hydroxybiphenyls: conformationally restricted structural probes, *Mol. Pharmacol.* 33 (1998) 120–126.

[2] G.M. Stancel, H.L. Boettger-Tong, C. Chiappetta, S.M. Hyder, J.L. Kirkland, Toxicity of endogenous and environmental estrogens: what is the role of elemental interactions? *Environ. Health Perspect.* 103 (1995) 29–33.

[3] H. Aldercreutz, H. Markkanen, W.S., Plasma Concentrations of phytoestrogens in Japanese men, *Lancet* 342 (1993) 1209–1210.

[4] B.S. Katzenellenbogen, Estrogen receptors: bioactivities and interactions with cell signaling pathways, *Biol. Reprod.* 54 (1996) 287–293.

[5] G.G.J.M. Kuiper, E. Enmark, M. Peltö-Huikko, S. Nilsson, J.-A. Gustafsson, Cloning of a novel estrogen receptor expressed in rat prostate and ovary, *PNAS* 93 (1996) 5925–5930.

[6] S. Mosselman, J. Polman, R. Dijkema,  $ER\beta$ : identification and characterization of a novel human estrogen receptor, *FEBS Lett.* 392 (1996) 49–53.

[7] G.G.J.M. Kuiper, B. Carlsson, K. Grandien, E. Enmark, J. Haggblad, S. Nilsson, J.-A. Gustafsson, Comparison of the ligand binding specificity and transcript tissue distribution of estrogen receptors { $\alpha$ } and { $\beta$ }, *Endocrinology* 138 (1997) 863–870.

[8] T.C. Register, M.R. Adams, Coronary artery and cultured aortic smooth muscle cells express mRNA for both the classical estrogen receptor and the newly described estrogen receptor  $\beta$ , *J. Steroid Biochem. Mol. Biol.* 64 (1998) 187–191.

[9] K. Paech, P. Webb, G.G.J.M. Kuiper, S. Nilsson, J.-A. Gustafsson, P.J. Kushner, T.S. Scanlan, Differential ligand activation of estrogen receptors  $ER\alpha$  and  $ER\beta$  at AP1 Sites, *Science* 277 (1997) 1508–1510.

[10] M.M. Montano, A.K. Jaiswal, B.S. Katzenellenbogen, Transcriptional regulation of the human quinone reductase gene by antiestrogen-liganded estrogen receptor $\alpha$  and estrogen receptor $\beta$ , *J. Biol. Chem.* 273 (1998) 25443–25449.

[11] S.R. Stauffer, C.J. Coletta, R. Tedesco, G. Nishiguchi, K. Carlson, J. Sun, B.S. Katzenellenbogen, J.A. Katzenellenbogen, Pyrazole ligands: structure-affinity/activity relationships and estrogen receptor- $\alpha$ -selective agonists, *J. Med. Chem.* 43 (2000) 4934–4947.

[12] D.S. Mortensen, A.L. Rodriguez, J. Sun, B.S. Katzenellenbogen, J.A. Katzenellenbogen, Furans with basic side chains: synthesis and biological evaluation of a novel series of antagonists with selectivity for the estrogen receptor  $\alpha$ , *Bioorg. Med. Chem. Lett.* 11 (2001) 2521–2524.

[13] G.A. Nishiguchi, A.L. Rodriguez, J.A. Katzenellenbogen, Diaryl-dialkyl-substituted pyrazoles: regioselective synthesis and binding affinity for the estrogen receptor, *Bioorg. Med. Chem. Lett.* 12 (2002) 947–950.

[14] A.J. Hopfinger, Computer-assisted drug design, *J. Med. Chem.* 28 (1985) 1133–1139.

[15] R.D. Cramer III, D.E. Patterson, J.D. Bunce, Comparative molecular field analysis (CoMFA). 1. Effect of shape on binding of steroids to carrier proteins, *J. Am. Chem. Soc.* 110 (1988) 5959–5967.

[16] J.P. Horwitz, I. Massova, T.E. Wiese, A.J. Wozniak, T.H. Corbett, J.S. Sebolt-Leopold, D.B. Capps, W.R. Leopold, Comparative molecular field analysis of in vitro growth inhibition of L1210 and HCT-8 cells by some pyrazoloacridines, *J. Med. Chem.* 36 (1993) 3511–3516.

[17] C.L. Waller, T.I. Oprea, A. Giolitti, G.R. Marshall, Three-dimensional QSAR of human immunodeficiency virus (I) protease inhibitors. 1. A CoMFA study employing experimentally-determined alignment rules, *J. Med. Chem.* 36 (1993) 4152–4160.

[18] G. Jones, P. Willett, R.C. Glen, Molecular recognition of receptor sites using a genetic algorithm with a description of desolvation, *J. Mol. Biol.* 245 (1995) 43–53.

[19] G. Jones, P. Willett, R.C. Glen, A.R. Leach, R. Taylor, Development and validation of a genetic algorithm for flexible docking, *J. Mol. Biol.* 267 (1997) 727–748.

[20] C. Bissantz, G. Folkers, D. Rognan, Protein-based virtual screening of chemical databases. 1. Evaluation of different docking/scoring combinations, *J. Med. Chem.* 43 (2000) 4759–4767.

[21] J. Åqvist, C. Medina, J.-E. Samuelsson, A new method for predicting binding affinity in computer-aided drug design, *Protein Eng.* 7 (1994) 385–391.

- [22] A.R. Ortiz, M.T. Pisabarro, F. Gago, R.C. Wade, Prediction of drug binding affinities by comparative binding energy analysis, *J. Med. Chem.* 38 (1995) 2681–2691.
- [23] C. Pérez, M. Pastor, A.R. Ortiz, F. Gago, Comparative binding energy analysis of HIV-1 protease inhibitors: incorporation of solvent effects and validation as a powerful tool in receptor-based drug design, *J. Med. Chem.* 41 (1998) 836–852.
- [24] P.R.N. Jayatilke, A.C. Nair, R. Zauhar, W.J. Welsh, Computational studies on HIV-1 protease inhibitors: influence of calculated inhibitor-enzyme binding affinities on the statistical quality of 3D-QSAR CoMFA models, *J. Med. Chem.* 43 (2000) 4446–4451.
- [25] A.C.W. Pike, A.M. Brzozowski, R.E. Hubbard, T. Bonn, A.-G. Thorsell, O. Engstrom, J. Ljunggren, J.-A. Gustafsson, M. Carlquist, Structure of the ligand-binding domain of oestrogen receptor beta in the presence of a partial agonist and a full antagonist, *EMBO J.* 18 (1999) 4608–4618.
- [26] A.M. Brzozowski, A.C.W. Pike, Z. Dauter, R.E. Hubbard, T. Bonn, O. Engström, L. Öhman, G.L. Greene, J.-Å. Gustafsson, M. Carlquist, Molecular basis of agonism and antagonism in the oestrogen receptor, *Nature* 389 (1997) 753–758.
- [27] Maestro, 5.0 ed., Schrödinger Inc., Portland, OR, 1998.
- [28] W.L. Jorgensen, D.S. Maxwell, J. Tirado-Rives, Development and testing of the OPLS all-atom force field on conformational energetics and properties of organic liquids, *J. Am. Chem. Soc.* 118 (1996) 11225–11236.
- [29] F. Mohamadi, N.G.J. Richards, W.C. Guida, R. Liskamp, M. Lipton, C. Caulfield, G. Chang, T. Hendrickson, W.C. Still, Macromodel—an integrated software system for modeling organic and bioorganic molecules using molecular mechanics, *J. Comput. Chem.* 11 (1990) 440.
- [30] D. Qiu, P.S. Shenkin, F.P. Hollinger, W.C. Still, The GB/SA continuum model for solvation. a fast analytical method for the calculation of approximate born radii, *J. Phys. Chem. A* 101 (1997) 3005–3014.
- [31] A.C. Wallace, R.A. Laskowski, J.M. Thornton, LIGPLOT: a program to generate schematic diagrams of protein–ligand interactions, *Protein Eng.* 8 (1995) 124–127.